J. Fluid Mech. (1985), *vol.* 152, *pp.* 455–478
Printed in Great Britain

Laser-Doppler anemometer measurements of turbulent structure in drag-reducing fibre suspensions

By W. D. McCOMB AND K. T. J. CHAN
School of Engineering, University of Edinburgh, Edinburgh EH9 3JL

(Received 7 February 1983 and in revised form 21 August 1984)

A laser-Doppler anemometer (LDA) was used to measure turbulent velocities in drag-reducing fibre suspensions. Measurements of streamwise velocities (and, in one case, the circumferential velocity as well) were made in flow through a straight pipe at $x/d = 190$, and at Reynolds numbers in the range 1.4×10^4–5.3×10^4. The fibres used were chrysotile asbestos of high aspect ratio ($\sim 10^5$), at a concentration of 300 w.p.p.m. They were dispersed in an aqueous solution of a surfactant (0.5% by weight Aerosol OT). In some experiments, the fibre suspensions were supplemented by a drag-reducing polymer (Separan AP30) at a concentration of 150 w.p.p.m. A complete experiment involved passing a quantity of fibre suspension through the apparatus a number of times (at a given Reynolds number) and measuring the velocity distribution across the pipe during each pass. As the amount of drag reduction generally declined with the number of passes (i.e. due to fibre degradation), this provided a convenient way of varying the percentage drag reduction as an experimental parameter. Results were obtained for mean velocity and intensity profiles, autocorrelations, and one-dimensional energy spectra. The mean period of turbulent bursts was determined by measuring autocorrelations with short sampling times.

At the lowest Reynolds number ($Re = 1.4 \times 10^4$), drag reductions of about 70% were obtained during the first two passes. This was accompanied by a reduction in the streamwise intensity below the level obtained in the surfactant solution alone. (Note: The opposite behaviour is found in drag-reducing polymer solutions, where intensity levels are larger than those in the solvent alone.) A measurement of the r.m.s. circumferential velocity showed an increased level (relative to surfactant alone) during this part of the experiment. During further passes, there was a transition to 'polymer-like' behaviour, with increased streamwise intensity, which subsequently declined with pass number (and hence drag reduction) towards the result for surfactant alone. This effect had previously been found in preliminary experiments at $Re = 9 \times 10^3$ (McComb & Chan 1979). Repetition of the experiment at $Re = 1.4 \times 10^4$, with the addition of Separan AP30, confirmed the existence of this transition from 'fibre-like' to 'polymer-like' drag reduction. In this case, the drag reduction was smaller (at about 60%), but the mixed suspension was much more resistant to degradation, with transition occurring at the ninth pass. However, such behaviour was not found at higher Reynolds numbers ($Re = 3.2 \times 10^4$ and 5.3×10^4), in fibre suspensions where increased streamwise intensities occurred, even at high levels of drag reduction (about 70%).

Anomalous streamwise autocorrelations were found during 'fibre-like' drag reduction but in the 'polymer-like' regime they were very similar to those measured in polymer solution, and showed characteristically increased lengthscales. On the other

hand, energy spectra were found to be anomalous in all cases and showed an energy deficit at lengthscales of the same order as the fibre length. Finally, mean bursting periods were found to be much increased, with the increases being about the same as those in polymer solutions at the same Reynolds number and percentage drag reduction.

1. Introduction

The aim of this study was to measure velocity distributions in aqueous suspensions of drag-reducing fibres. One of our main objectives was to investigate the differences between the effect produced by macroscopic fibres and the better-known effect found in solutions of microscopic polymer molecules. We begin by reviewing the background to our work. In particular, we shall briefly discuss drag reduction by polymers, drag reduction by macroscopic fibres, and what is known at present of the relationship between the two effects.

Drag reduction in polymer solutions has been defined as the reduction of skin friction in turbulent flow below that of the solvent alone (Lumley 1969). It has been demonstrated in many flow situations, but by far the most important is that of well-developed two-dimensional mean flow in pipes or channels. Under these circumstances, drag reduction can be defined in terms of a reduction in pressure drop (due to additives) at the same flow rate. Or

$$DR = \frac{\Delta P_s - \Delta P_a}{\Delta P_s} \times 100\,\%, \tag{1}$$

where DR stands for drag reduction (as a percentage), ΔP_s is the streamwise pressure drop in the solvent and ΔP_a is the pressure drop at the same flow rate with the additive present.

Interest in this subject was stimulated by the discovery that certain long-chain polymers (both natural and synthetic) could reduce turbulent drag by quite large amounts, even when present in rather small concentrations. For example, a typical effective polymer can reduce drag by about 70 % at a concentration by weight of only 5 p.p.m. This is a truly remarkable phenomenon. It is not, therefore, particularly surprising that there have been several hundred investigations of pressure drop–flow rate relationships in a variety of polymer solutions and experimental situations. There has also been a somewhat smaller number of studies which attempt to interpret the phenomenon in terms of changes in the underlying turbulent structure. But, with the exception of some flow-visualization techniques – which in the main really only give qualitative results – such investigations have faced the problem that the non-Newtonian nature of the polymer solutions introduces ambiguities into measurement techniques which are well-established for water flows.

A probable exception to this general criticism would be the use of laser anemometry. Unfortunately there have only been a few investigations using LDA, and of these, most have lacked general validity because of either the complex nature of the flow studied (e.g. Rudd 1972; Logan 1972) or limitations in the LDA system used (e.g. Chung & Graebel 1972; Mizushima & Usui 1977). Two studies would seem to be free from these strictures. Reischman & Tiederman (1975) made LDA measurements of axial velocity in a 2-dimensional channel and found increased turbulent intensities in dilute polymer solutions (as did Rudd (1972) and Logan (1972) – but there were some detailed differences in the shapes of the profiles). More recently, McComb &

Rabie (1982) have used LDA to measure axial velocities in pipe flow, where the drag reduction was produced by injecting concentrated polymer solutions at the centreline or the wall. Despite the different method of producing drag reduction, the results for axial velocity and turbulence profiles seem to agree quite well with those of Reischman & Tiederman (1975).

We shall not give a full discussion of the polymer effect here. Reference may be made to the papers cited, and to some of the excellent reviews available (e.g. Hoyt 1972*a*, 1977; Little *et al.* 1975; Virk 1975). For our purposes, it will be sufficient to summarize what is known about changes in turbulent structure due to polymer additives. To do this, we have to begin by stating that, in terms of quantitative results and rigorous comparisons of like with like, the situation is hardly satisfactory. Yet if we take the broad qualitative agreement of four of the LDA investigations (Rudd 1972; Logan 1972; Reischman & Tiederman 1975; McComb & Rabie 1982) both with each other and with the many flow-visualization studies, then we may make the following statements about turbulent structure in polymer solutions (when compared to results for solvent alone): (*a*) it seems virtually beyond doubt that integral length- and timescales are increased, as is the mean period between bursts; (*b*) it seems very probable that axial turbulent intensity is increased, particularly near the wall; (*c*) it seems quite probable that spanwise and radial intensities are reduced.

Turning now to the study of macroscopic fibre suspensions, we find quite a different situation. Investigations of turbulent flow in such suspensions have generally been carried out as an adjunct to specific industrial processes, and tend to be reported in specialist journals associated with certain industries such as paper-making or synthetic textiles. Where drag reduction occurs it is usually a relatively small effect (typically of order 20 %) and requires relatively large fibre concentrations (typically a few percent, by weight). Such work was (and still is) often reported without reference to the huge literature on polymer drag reduction.

The scientific interest of this phenomenon was greatly enhanced by the discovery of Ellis (1970) that certain asbestos fibres (prepared by Turner Brothers Asbestos Co. Ltd) could give high drag reductions (44 %) in dilute suspensions (100 p.p.m. by weight). Crucial features were the very high length-to-diameter ratio (or aspect ratio) of the fibres and the use of a surfactant to ensure that they were well dispersed. From our present point of view, the importance of this result is that it is quite comparable to results obtained with polymer additives. Subsequent, more extensive, investigations (Hoyt 1972*b*; Radin, Zakin & Patterson 1975) have confirmed the effectiveness of the TBA asbestos fibres.

An additional feature of considerable interest is the result of combining both macroscopic fibres and drag-reducing polymers in the one suspension. Lee, Vaseleski & Metzner (1974) found that when both types of additive were used together they reduced drag by amounts greater than the sum of the two independent effects. In particular, drag reductions greater than 95 % were obtained in suspensions containing TBA asbestos fibres and Separan AP30 (a drag-reducing polyacrylamide). They also found that the mixed suspensions were much less susceptible to degradation under shear. These effects have been confirmed by Sharma, Seshadri & Malhotra (1979), who reported similar behaviour when TBA asbestos fibre suspension was injected into pipe flow of drag-reducing polymer solution.

Let us now consider the question of whether polymers and fibres reduce drag by different mechanisms. In other words, do they modify or change the turbulence in different ways?

Superficially, the answer to that question might appear to be 'no'. If we compare

the two effects on the basis of additive characteristics, they really look quite similar. Thus:

Polymers should be:

(*a*) Of very long chain structure, with little branching (correspondingly the molecular weight should be large; typically about 10^6).

(*b*) Flexible.

(*c*) Well dissolved.

Fibres should be:

(*a*) Very long and thin (probably the aspect ratio must be greater than 25 and best results have been obtained with a value of order 10^5).

(*b*) Flexible.

(*c*) Well dispersed (a surfactant may be necessary).

Of course a comparison of the two additives in terms of the way in which drag reduction depends on the flow (i.e. onset relationships, dependence on system size, dependence on Reynolds number) might suggest differences between the two effects. But here there are so many inconsistencies (and indeed the difficulty of distinguishing differences of kind from those merely of degree) that one is thrown back on considerations of the turbulent structure.

Measurements of turbulent structures in drag-reducing fibre suspensions are thin on the ground. Bobkowicz & Gauvin (1967) have used a tracer technique to study drag-reducing nylon fibre suspensions and have reported increased radial turbulent intensity. LDA measurements on wood pulp suspensions have been made by Ek, Moller & Norman (1979) and Kerekes & Garner (1982). In both cases reduced streamwise turbulent intensities were found, although Ek *et al.* did observe increased intensities towards the pipe wall. Clearly these results suggest that fibres and polymers *do* modify turbulence in different ways. Our own preliminary results for TBA asbestos fibres at $Re = 9 \times 10^3$ (McComb & Chan 1979) also show reduced streamwise intensity levels. However, after several passes through the apparatus, the streamwise intensity increased above the level for the surfactant solution alone but thereafer declined with increasing number of passes. Thus we were led to postulate a transition from a 'fibre-like' mechanism to a 'polymer-like' mechanism for drag reduction. In the rest of this paper we will be concerned with a more comprehensive investigation of this effect. Finally, for completeness, we should mention our preliminary report of spectral measurements (McComb & Chan 1981): this will be discussed later.

2. Experimental apparatus and methods

2.1. *The flow system*

The flow system is shown schematically in figure 1 and was of the 'blow down' type. Suspensions were prepared in the header tank and allowed to flow under gravity into the pressure tank. Air pressure (20 p.s.i.g.) was used to propel the suspensions through a horizontal pipe of 2 cm nominal bore and then through a return line to the header tank. Flow rates were controlled by a constant-flow valve. The actual flow rate was determined by timing the change in levels on a sight-glass in the header tank.

The main flow pipe was made of Perspex and was 380 cm long with an internal diameter of 1.95 cm. Pressure tappings, 3 mm in diameter, were located at intervals of 60 cm. The relatively large diameter of the tappings was intended to prevent clogging by the fibres and frequent checks were made to ensure that this did not happen. Pressure drops were measured using a liquid-in-glass manometer with a

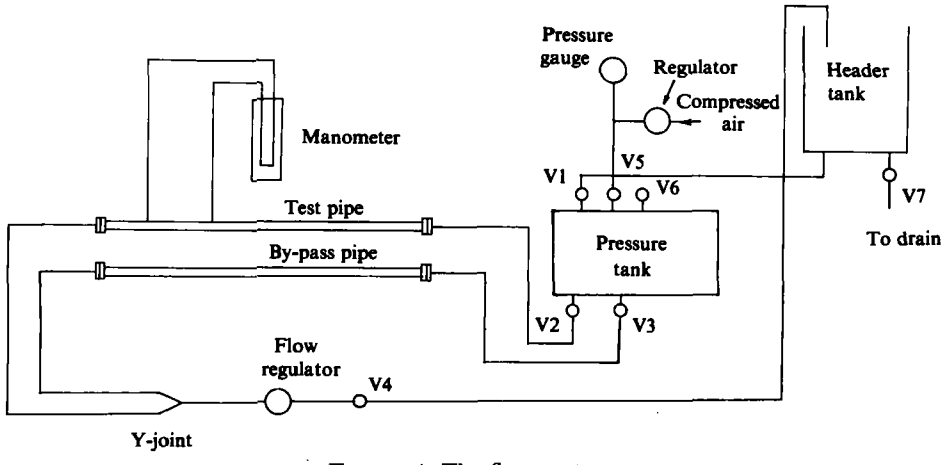

FIGURE 1. The flow system.

liquid of specific gravity 1.58 at a temperature of 20 °C. The test section of the pipe was located 154 diameters from the inlet to ensure well-developed flow.

An essential feature of this investigation was the re-cycling of each suspension through the apparatus a number of times, so that the effect of degradation could be studied. A by-pass pipe was incorporated (see figure 1) which did not have pressure tappings but was otherwise identical with the main flow pipe. This allowed the pressure tank to be emptied after the completion of an experimental run and the residual suspension to be returned to the header tank.

2.2. *LDA for measurement of streamwise velocities*

The LDA was used in the real-fringe, forward-scattering mode. This arrangement was chosen for its ease of alignment and the ability to combine high spatial resolution with good signal-to-noise ratio.

The optical arrangement is shown in figure 2 and the various components have been described elsewhere (McComb & Rabie 1982). In this application, the angle between the beams was 20.86° which resulted in the parameters of the probe volume being as follows:

(*a*) The fringe spacing was 1.74 μm.

(*b*) The probe volume dimensions were $0.03 \times 0.17 \times 0.03$ mm, the longest dimension being along the radius of the pipe.

(*c*) For this configuration, the Doppler frequency f_0 was 575 kHz for a velocity of one m s^{-1}.

2.3. *LDA for measurement of transverse velocities*

The optical arrangement for this LDA is shown in figure 3. Like the streamwise LDA, the real-fringe, forward-scattering mode was used. However, the measurement of the transverse (or circumferential) component of the fluctuating velocity introduces a number of new features. Thus:

(*a*) In the absence of secondary flows, there is no mean velocity in the spanwise direction. Thus the velocity fluctuates about zero and the d.c. level of the LDA signal spectrum must be offset. This was accomplished using a proprietary device (the DISA Flow Direction Adapter) which uses a pair of Bragg cells to impose a fixed frequency shift on the system (i.e. the fringes move and the fluid velocity fluctuations may be measured relative to the 'fringe velocity').

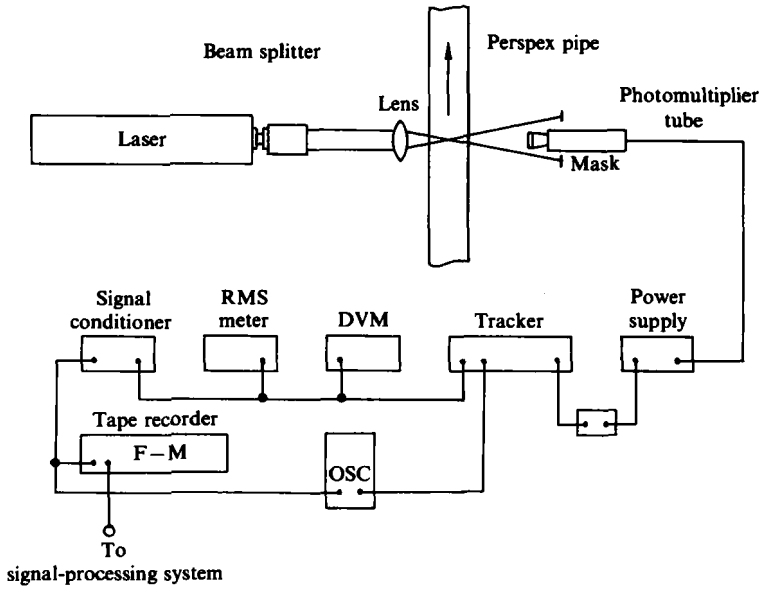

FIGURE 2. Optical arrangement for measurement of axial velocities.

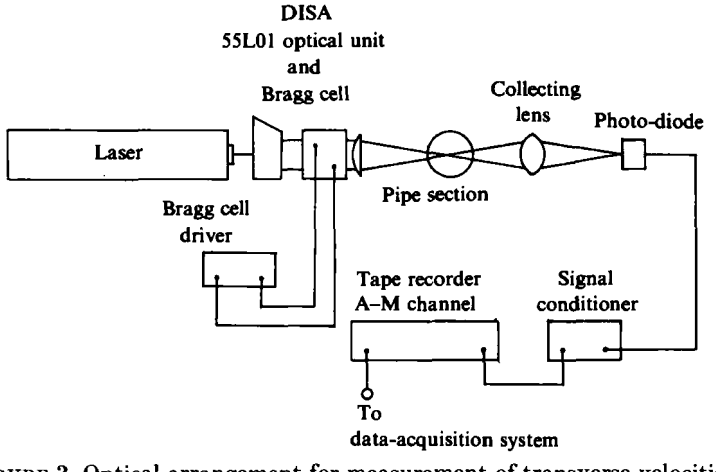

FIGURE 3. Optical arrangement for measurement of transverse velocities.

(*b*) It may be seen from figure 3 that in this configuration the pipe wall will act as a lens (strictly, the air–Perspex and the Perspex–water interfaces act as lenses). Thus the intersection angle of the beams, along with the apparent distance of the probe volume from the wall, will not take the same value as in air. These effects have to be taken into account when making measurements at successive radial positions. Also, a great deal of extra care had to be taken over alignment as this was much more critical than in the streamwise case.

(*c*) Mixing of incident and reflected beams resulted in a 'spike' in the signal spectrum at the shift frequency. This ruled out the use of a frequency tracker. Therefore values of the r.m.s. transverse fluctuation had to be obtained from the width of the a.c. peak in the signal spectrum – a relatively slow and time-consuming procedure.

The laser used was a 5 mW He–Ne Spectra Physics Model 120, as in the streamwise measurements. The beam splitter (DISA 55L01) and the DISA Flow Direction Adapter formed an integrated unit with a fixed beam separation of 50 mm and the parallel beams were focused to form a moving fringe pattern at the measuring point using a lens with a focal length of 300 mm. A lens with a focal length of 130 mm was used to collect scattered light, which was then focused on a photodiode.

The angle at which the beams intersected varied between a maximum value of 9.52° (in air) to a minimum of 6.92° (in water, at the pipe wall nearest to the laser). For these two extremes, parameters of the probe volume were as follows:

Beam intersection angle = 9.52°:

(*a*) the fringe spacing was 3.8 μm;

(*b*) the probe volume dimensions were $0.18 \times 2.25 \times 0.18$ mm^3, the longest dimension being along the radius of the pipe;

(*c*) the Doppler frequency f_D was 263 kHz for a velocity of one m s^{-1}.

Beam intersection angle = 6.92°:

(*a*) the fringe spacing was 5.24 μm;

(*b*) the probe volume dimensions were $0.18 \times 3.0 \times 0.18$ m^3, the longest dimension being along the radius of the pipe;

(*c*) the Doppler frequency was 191 kHz for a velocity of 1 m s^{-1}.

2.4. *Data acquisition and analysis*

The signal-processing chains for the two LDA systems are shown, along with their respective optical arrangements, in figures 2 and 3. For the streamwise velocity measurements, a frequency tracker (Communications and Electronics Ltd, model HF) was used to convert the Doppler frequency from the photomultiplier into a voltage proportional to the instantaneous velocity. Mean and r.m.s. velocities were obtained using digital and r.m.s. voltmeters. The instantaneous voltage from the tracker was also recorded on a Racal-Thermionic Store 4D tape recorder. Recorded signals were played back (at recording speed) through a low-pass filter, with a cut-off frequency of 5 kHz. Autocorrelations (and hence the mean bursting period) were obtained using a correlator (Hewlett-Packard 3721A).

The output from the low-pass filter was also digitized at a rate of 10 kHz, using an A/D converter and PDP8 minicomputer. The digitized data were transferred to the ICL 4/75 computer, where energy spectra were calculated using the Fast Fourier Transform algorithm. This system for obtaining the spectrum is essentially the same as that described previously in the paper by McComb, Allan & Greated (1977), where discussions of ambiguity noise levels and spectral-resolution limits will also be found.

In the case of the LDA for transverse velocity measurements, the imposed frequency shift was limited by the frequency response of the tape recorder (flat to 300 kHz at the fastest recording speed). This was chosen to be 250 kHz, resulting in a Doppler signal with beat frequency fluctuating about 250 kHz. This was processed using the computer-based system described in the preceding paragraph. As the A/D converter could only sample data at a rate of 110 kHz, the output from the low-pass filter was recorded at the highest tape speed and played back at the lowest. This reduced the Doppler signal centre frequency by a factor of 16 to 15.63 kHz, which was then digitized at a sampling rate of 40 kHz.

2.5. *Seeding of the flow*

At first we added small amounts of milk to seed the flow, following our previous practice with polymer solutions. However, this was found to be unnecessary. In the

course of tests aimed at clarifying our interpretation of the LDA signal, it was discovered that the surfactant (Aerosol OT) provided adequate seeding. This was presumably due to naturally occurring micelles. These points will be given a fuller discussion in §3.2.

3. Preliminary tests

3.1. *Tests with water flows*

As a first test of the apparatus, values of the friction factor were obtained over a range of Reynolds numbers, 2×10^3–6×10^4, for water and for a 0.5% Aerosol OT solution. In both cases, the results agreed with the well-known Blasius formula (within $\pm 1\%$). From this we could conclude that the turbulent flow in the test section was fully developed, and that the Aerosol OT did not affect the turbulent friction (in agreement with the results of Ellis 1970; Hoyt 1972*b*; Lee *et al.* 1974 and Moyls & Sabersky 1978).

In order to check the performance of the two LDA systems, measurements were made in water flow and in solutions of Aerosol OT, for the range of Reynolds numbers 1×10^4–5×10^4. Details can be found in the thesis by Chan (1980). However, results for mean and r.m.s. velocity profiles, one-dimensional energy spectra and correlation coefficients were in satisfactory agreement with those available in the literature. Also, in the figures to be given below, a curve for water alone is generally included for purposes of comparison.

3.2. *Interpretation of the LDA signal*

The use of LDA in fibre suspensions raises an important question about the interpretation of the output signal. Assuming that we have an appropriate seeding material present, in general we should expect that the LDA signal will consist of contributions from both the fluid motion and the fibre motion. The question then is: to what extent can we obtain unambiguous information about the fluid motion?

To try to answer this question we carried out a number of experiments, which we shall now discuss.

To begin with, we studied the LDA signal by photographing oscilloscope traces of the photocurrent. Measurements were made in water alone, in water with 100 w.p.p.m. of milk, in water with 200 w.p.p.m. of milk, and in a 0.5% aqueous solution of Aerosol OT. For water alone there was no detectable Doppler signal and the photograph showed only background noise. For both concentrations of milk, Doppler 'bursts' of good quality were observed. However, in the case of the Aerosol OT solution, there was a perfectly adequate LDA signal. The appearance of this signal suggested that there were many more scattering particles in the probe volume than had been the case with either concentration of milk.

The above experiments were repeated with fibre present (at 300 w.p.p.m.) and with fibre and polymer (150 w.p.p.m. Separan AP30). In no case did the signal differ from the result obtained with Aerosol OT alone. There was no evidence of any additional contribution from milk particles or from fibres.

The preceding results were obtained from 'first passes' of the fibre suspension. We also checked the appearance of the Doppler photocurrent over a number of passes of one fibre suspension. If there were any contribution from the fibres, then one could expect this to change as the fibre suspension degraded. Yet after five passes of the suspension through the apparatus, the appearance of the Doppler signal was unchanged. Full details of these tests will be found in the thesis by Chan (1980).

One would like to put this on a more quantitative footing, but unfortunately there

are too many imponderables in comparing Doppler signal spectra from drag-reducing turbulent flows. However, we did carry out a preliminary experiment, using the streamwise LDA to measure the centreline velocity in laminar flow through a pipe of 5 mm internal diameter. Measurements were made in tap water, Aerosol OT solution, and Aerosol OT solution containing fibres at a concentration of 100 w.p.p.m. No signal was detected from water alone. A comparison of photocurrent spectra for the other two fluids revealed no evidence of spectrum broadening or reduced signal-to-noise ratio in the fibre suspension.

In all, therefore, the fibres do not seem to contribute to the Doppler signal. It is tempting to try to understand this in terms of fibre properties. Suppose we assume that the suspension is well dispersed so that we may think in terms of the behaviour of individual fibres (sometimes referred to as fibrils). Then we may consider two extreme cases. First, if the fibres are fully stretched out, they may be taken to have a mean diameter of 0.05 μm and thus their light-scattering efficiency will be small. In fact it is about 0.05, according to data tabulated by Wickramasinghe (1973), which may be compared with about 4 for a spherical fat particle in milk. Also, their length of 1.4 mm compared to the LDA probe volume dimension of 0.03 mm, suggests that in most orientations they would tend to bridge across the fringes. Thus, a small contribution to the a.c. part of the signal seems a not unreasonable result. Secondly, if the individual fibre is fully coiled up into a small ball, then the mean diameter would be less than 1.6 μm. This would make it a reasonable (if not good) seeding material for the purpose of LDA. However, it has to be said that the drag-reducing suspensions used look very much like diffuse cotton wool flowing down the pipe. So a mesh of entangled, extended fibres seems a more plausible picture.

Let us turn now to the use of Aerosol OT as a seeding material. As this chemical must be present in order to disperse the fibres, then the above tests show that we have little choice in the matter: the main part of the LDA signal arises from the micelles of Aerosol OT. Measurements were made in water (with milk as a 'seed') and in 0.5 % Aerosol OT solutions. Results for means and r.m.s. velocity profiles were in good agreement, as were one-dimensional energy spectra and correlation coefficients in the two fluids. The results may be found in the thesis by Chan (1980). We concluded therefore that Aerosol OT was a satisfactory seeding material for LDA.

3.3. *Drag-reducing fibre suspensions*

As mentioned earlier, some preliminary measurements were made at $Re = 9.0 \times 10^3$ in a 300 w.p.p.m. fibre suspension. Mean and r.m.s. profiles of the axial velocity have been presented elsewhere (McComb & Chan 1979). In this experiment the LDA output signal was not recorded and consequently neither energy spectra nor correlation coefficients were obtained. The drag reduction obtained was quite large, at 63 % for the first two passes. Thereafter it declined with pass number, as degradation took place.

The most interesting feature of these results, was the apparent transition between two forms of behaviour, as the suspension degraded. In the first two passes, the mean velocity profiles lay beyond the ultimate profile of Virk, Mickley & Smith (1970) for polymer solutions, and indeed resembled a profile for laminar flow. In successive passes thereafter, the profiles lay within the ultimate profile for polymer drag reduction and showed a trend back to the result for water, as the amount of drag reduction decreased. A transition from one kind of mechanism to another would be only one of several explanations for this effect. But the behaviour of the turbulent intensity profiles seemed to be conclusive evidence for transitional behaviour. In the

first two passes, the turbulent intensity was everywhere less than in water at the same Reynolds number. In subsequent passes, it was generally greater than in water (except, perhaps, close to the wall) and showed a trend back to the Newtonian result as the amount of drag reduction declined.

Finally, in the light of the above discussion of preliminary results, we should define some nomenclature for the rest of this paper. Accordingly, we shall refer to each pass of a given fluid through the apparatus by its pass number, i.e. 'Pass 1', 'Pass 2' etc. The form of behaviour found in Pass 2 at $Re = 9.0 \times 10^3$, will be referred to as 'fibre-like'. The form of behaviour found in subsequent passes will be described as 'polymer-like'.

4. Results

4.1. *Drag reduction*

Measurements were made at Reynolds numbers of $Re = 1.4 \times 10^4$, 3.2×10^4 and 5.3×10^4. Experimental results were always taken in steady conditions, avoiding the beginning and end of each run. Reynolds numbers were calculated from the pipe diameter, the bulk mean velocity and the kinematic viscosity of water. All the suspensions used contained Aerosol OT, at a concentration of 0.5% by weight, and chrysotile asbestos fibre, at a concentration of 300 p.p.m. by weight. One main set of measurements was made in a fibre suspension at each of the three Reynolds numbers, using the pass number as an experimental parameter. An additional set of measurements at $Re = 1.4 \times 10^4$ was made on a fibre suspension containing also a drag-reducing polyacrylamide (Dow Chemicals Separan AP30; concentration 150 w.p.p.m.). The resultant reductions in friction drag for all these tests are summarized in table 1, together with those of the preliminary tests at a Reynolds number of 9.0×10^3.

In addition, as part of the process of studying the influence of the suspended fibres on the LDA signal (see §3.2), some rather short supplementary experiments were carried out at a Reynolds number of 1.4×10^4. These experiments were relatively incomplete in that only a few runs were made, and velocity measurements were only taken at a few radial positions. Results from two of the more complete of these experiments are also included in table 1.

From the table, it can be seen that the results for drag reduction were much as one would expect for these very effective asbestos fibres. The amounts of drag reduction were large, and degradation (i.e. reduction in effectiveness with pass number) was appreciable from the second or third pass onwards. In contrast, the fibre/polymer mixture was resistant to degradation up to the eighth pass. The peak amounts of drag reduction in the fibre suspension (over 70%) in several cases appear to be the largest values reported for these fibres in flow through smooth pipes, although Moyls & Sabersky (1978) have reported drag reductions greater than 80% in rough pipes.

In figure 4 results for several different pass numbers are plotted on a diagram of friction factor versus Reynolds number. The continuous lines are the usual correlations for flows of water in the laminar and turbulent regimes. The maximum drag reduction asymptote (Virk *et al.* 1970) is also drawn on the figure for reference, and for $Re = 9.0 \times 10^3$ and $Re = 1.4 \times 10^4$, it may be seen that the friction factor in the first two passes lay either on or below this asymptote for polymer solutions. Another noteworthy point is that a line drawn through the points for any of the passes shown, would pass through a minimum and subsequently tend to the line for water flows. This behaviour has also been observed by Moyls & Sabersky (1978).

Pass \ *Re*	9×10^3	1.4×10^4				3.2×10^4	5.3×10^4
	fibre	fibre			fibre + polymer	fibre	fibre
1	63	69	69	74	50	71	54
2	63	76	58	54	58	62	52
3	58	56	46	51	61	58	47
4	44	55	38	43	58	58	46
5	32	51			65	56	49
6	43	48			62	51	43
7	34	48			59	50	43
8	26	44			59	50	41
9	30	44			51	47	40
10	22	42			45	46	40
11		42			43		
12		39			41		
13		38			40		

TABLE 1. Summary of the results for drag reduction (expressed as a percentage). Note: (*a*) All suspensions contained TBA chrysotile asbestos fibre (300 w.p.p.m.) dispersed in an aqueous solution of Aerosol OT (0.5% by weight). (*b*) The mixed suspension also contained Separan AP30 (150 w.p.p.m.).

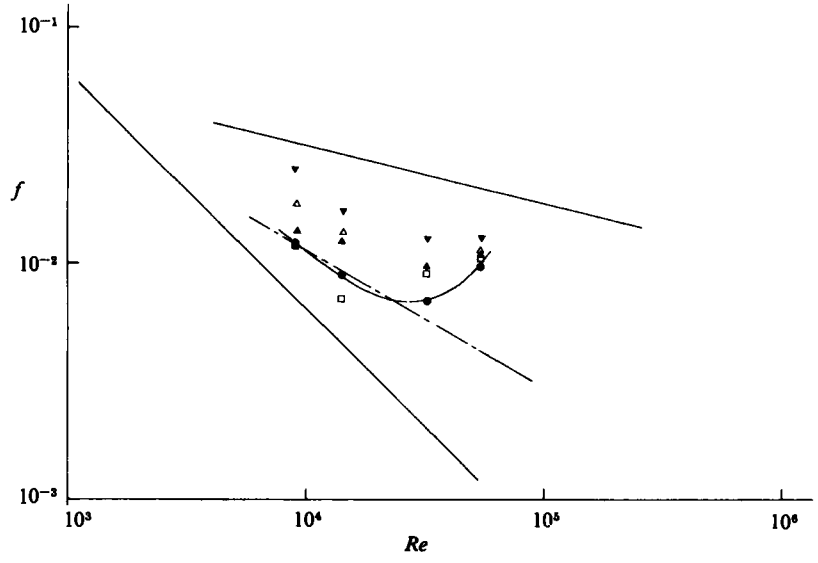

FIGURE 4. Friction factor versus Reynolds number diagram for flows in drag-reducing fibre suspensions: ●, Pass 1; □, Pass 2; ▲, Pass 3; △, Pass 4; ▼, Pass 10; ——, water; – – –, ultimate drag-reducing asymptote (Virk *et al.* 1970). Fibre concentration 300 p.p.m.

4.2. *Mean and r.m.s. velocity profiles*

Mean velocity profiles were plotted on semi-logarithmic scales as $U^+ = U/u^*$ against distance from the pipe wall $y^+ = yu^*/\nu$, where u^* is the friction velocity and ν the kinematic viscosity of water. The results are presented in figures 5–7 for the fibre suspensions at the three different Reynolds numbers, and in figure 8 for the fibre/polymer mixture. The r.m.s. velocity u (divided by u^*) was plotted against distance from the pipe wall y (divided by the pipe radius R) and results corresponding to the above mean velocity profiles are presented in figures 9–12. Also, some

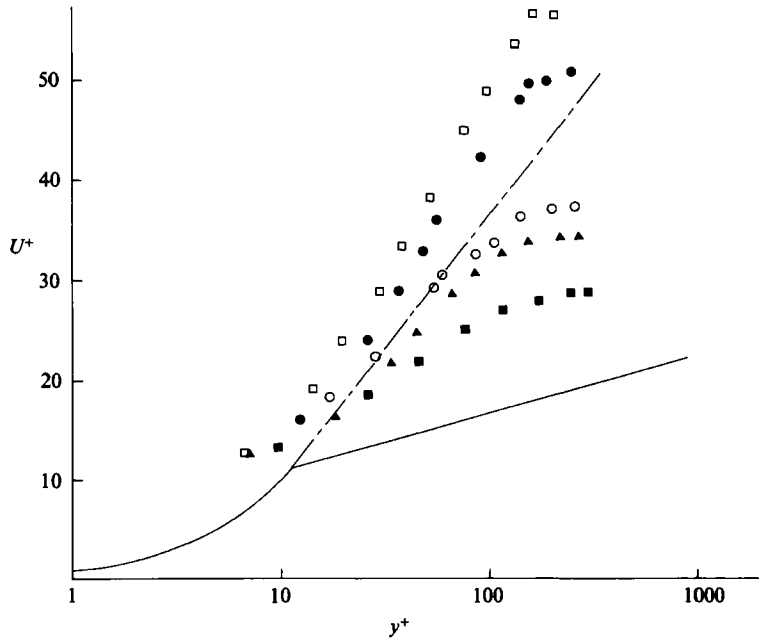

FIGURE 5. Mean velocity distributions in fibre suspension at $Re = 1.4 \times 10^4$: ●, Pass 1 $DR = 69\%$; □, Pass 2 $DR = 76\%$; ○, Pass 3 $DR = 56\%$; ▲, Pass 4 $DR = 55\%$; ■, Pass 10 $DR = 42\%$; ——, water; – – –, ultimate drag-reduction asymptote (Virk *et al.* 1970). Fibre concentration 300 p.p.m.

measurements of the circumferential velocity w in a fibre suspension at $Re = 1.4 \times 10^4$ are shown plotted against y/R in figure 13.

In the mean velocity diagrams, for purposes of comparison we show the conventional profile for a Newtonian fluid and the ultimate profile for drag-reducing polymer solutions (Virk *et al.* 1970). The former is given by $U^+ = y^+$ in the viscous sublayer and by $U^+ = 2.5 \ln y^+ + 5.5$ in the logarithmic region. The latter is given by $U^+ = 11.7 \ln y^+ - 17.0$.

Referring to figures 5–7, we see that the results for $Re = 1.4 \times 10^4$ are similar to the preliminary results taken at $Re = 9.0 \times 10^3$ (McComb & Chan 1979) in that the mean velocities for the first two passes lie beyond the Virk asymptote. This is not the case for the two higher Reynolds numbers, where all the profiles lie within this asymptote and there is thus no evidence of transitional behaviour. This difference between the two sets of Reynolds numbers (9.0×10^3, 1.4×10^4 and 3.2×10^4, 5.3×10^4) is underlined by two observations. First, for the higher Reynolds numbers, velocity profiles at the same percentage drag reduction are similar and hence are independent of Reynolds number. This was not the case at the two lower Reynolds numbers. Secondly, the mean velocity profile for $Re = 5.3 \times 10^4$, Pass 9 with $DR = 40\%$, agrees quite closely with that measured by Reischman & Tiederman (1975) in a polymer solution at $Re = 5.25 \times 10^4$ with $DR = 35.3\%$.

The results for the fibre/polymer mixture, as shown in figure 8, indicate that the experimental points for the 'undegraded' passes cluster together. Although they are close to the ultimate drag reduction asymptote, they lie within it. Thus it is not entirely clear from this figure that we are seeing the 'fibre-like' drag-reduction effect that would be the case in the pure fibre suspension at the same Reynolds number. It will be seen shortly that the turbulence data will help to give a clearer picture of the situation in the mixed suspension.

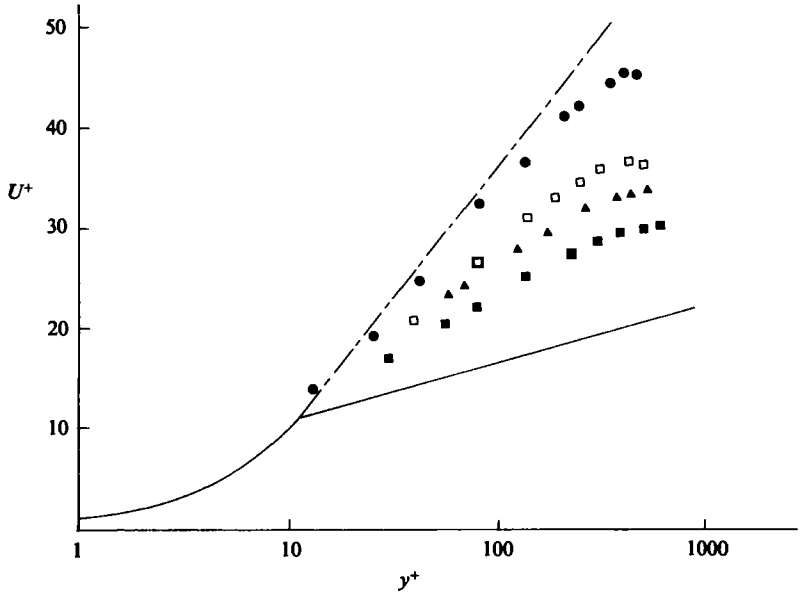

FIGURE 6. Mean velocity distributions in fibre suspension at $Re = 3.2 \times 10^4$: ●, Pass 1 $DR = 71\%$; □, Pass 2 $DR = 62\%$; ▲, Pass 4 $DR = 58\%$; ■, Pass 10 $DR = 46\%$; ——, water; – – –, ultimate drag-reduction asymptote (Virk *et al.* 1970). Fibre concentration 300 p.p.m.

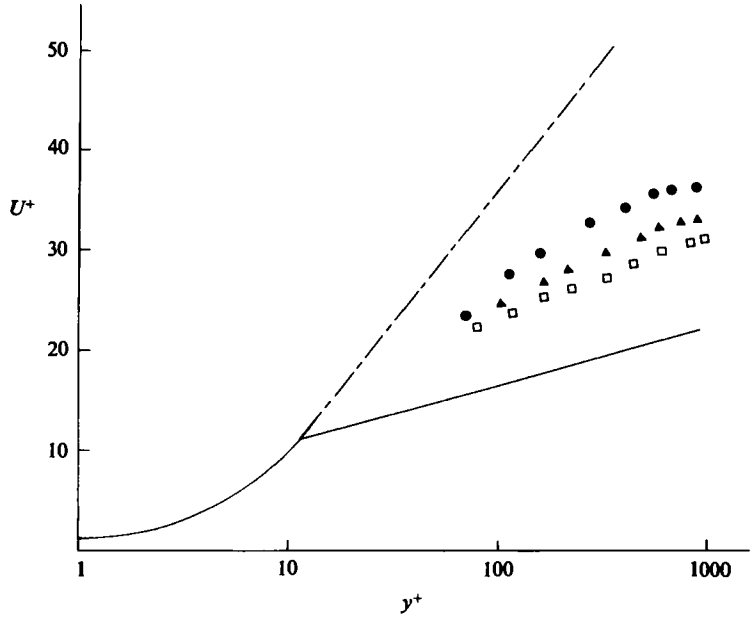

FIGURE 7. Mean velocity distributions in fibre suspension at $Re = 5.3 \times 10^4$: ●, Pass 1 $DR = 54\%$; △, Pass 3 $DR = 47\%$; □, Pass 9 $DR = 40\%$; ——, water; – – –, ultimate drag-reduction asymptote (Virk *et al.* 1970). Fibre concentration 300 p.p.m.

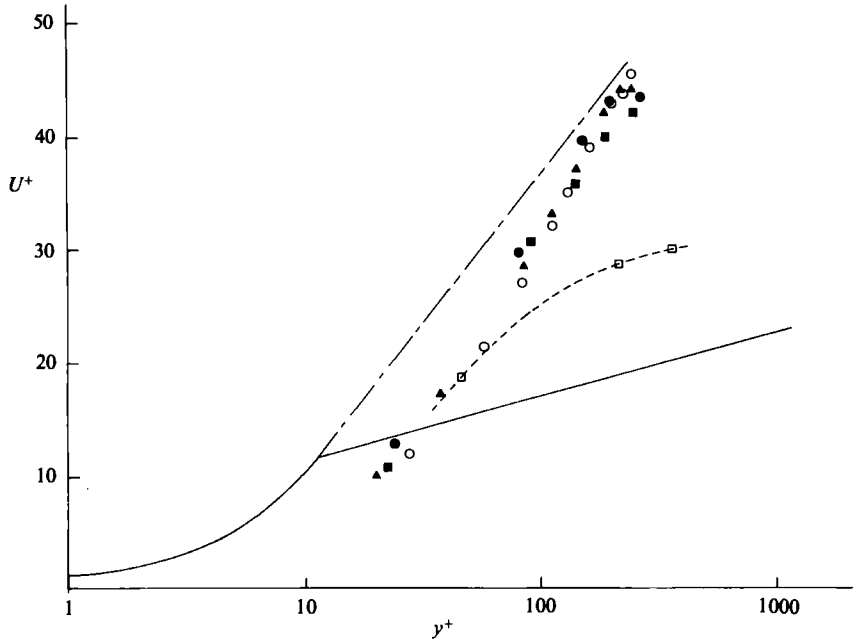

FIGURE 8. Mean velocity distributions in a mixed fibre/polymer suspension at $Re = 1.4 \times 10^4$: ●, Pass 1 $DR = 50\%$; ■, Pass 2 $DR = 58\%$; ▲, Pass 3 $DR = 61\%$; ○, Pass 8 $DR = 59\%$; □, Pass 13 $DR = 40\%$; ——, water; – – –, ultimate drag-reduction asymptote (Virk *et al.* 1970). 300 p.p.m. fibre + 150 p.p.m. polymer.

Before considering the r.m.s. velocity profiles, we should note that the mean velocity profiles for Pass 1 and Pass 2, at $Re = 1.4 \times 10^4$, show a distinct resemblance to the profile for laminar flow (e.g. see Bertshy & Abernathy 1977). This was also the case with the preliminary results at $Re = 9.0 \times 10^3$, where we have already seen that there was a marked reduction in streamwise turbulence, except at $y/R \simeq 0.3$ where the peak value was close to that for water. Reduced streamwise turbulence levels were also found in the various experiments carried out at $Re = 1.4 \times 10^4$. In figure 9 we present some results which closely resemble the behaviour found at $Re = 9.0 \times 10^3$, only here the peak value at $y/R = 0.3$ during Pass 1 actually exceeds the value in water.

For the two higher Reynolds numbers, figures 10 and 11 show that the results all lie in the polymer-like regime. In contrast, figure 12 shows that the intensities for the undegraded passes in the fibre/polymer mixture are all reduced below the value for water. That is, in the fibre-like regime. Paradoxically, the addition of drag-reducing polymer appears to stabilize the fibre-like effect against degradation.

Finally, some measurements of the circumferential turbulent r.m.s. velocity w are presented in figure 13, for $Re = 1.4 \times 10^4$ in a fibre suspension. Normally one would plot w/u^*, but this would shown an increase due to the reduction in u^*. Thus we have plotted the absolute r.m.s. level to show that this has increased. Therefore, it would be incorrect to interpret the fibre-like effect as simply a suppression of the turbulence. Clearly, if u has decreased in value while w has increased, the turbulence has been profoundly modified in some fashion.

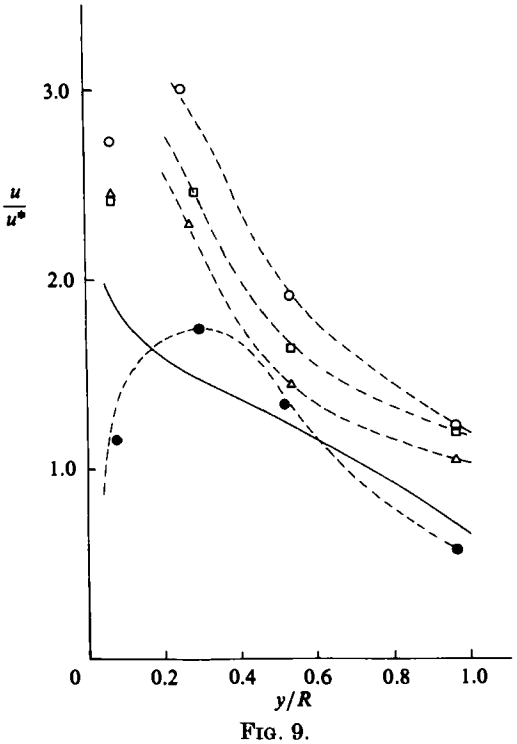

FIG. 9.

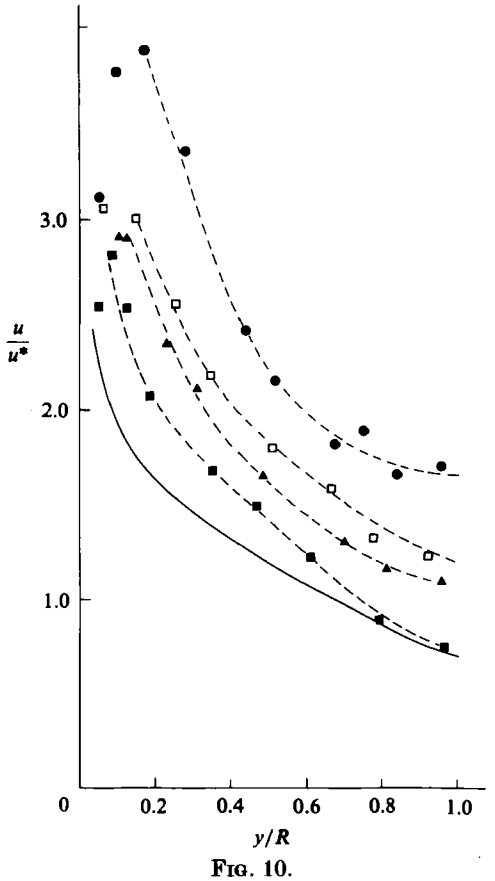

FIG. 10.

FIGURE 9. Axial turbulent intensities in fibre suspension at $Re = 1.4 \times 10^4$: ●, Pass 1 $DR = 69\%$; ○, Pass 2 $DR = 58\%$; □, Pass 3 $DR = 46\%$; △, Pass 4 $DR = 38\%$; ——, water.

FIGURE 10. Axial turbulent intensities in fibre suspension at $Re = 3.2 \times 10^4$. ●, Pass 1 $DR = 71\%$; □, Pass 2 $DR = 62\%$; ▲, Pass 4 $DR = 58\%$; ■, Pass 10 $DR = 46\%$; ——, water.

4.3. *One-dimensional energy spectra*

One-dimensional energy spectra were obtained using the FFT algorithm to compute spectra in the frequency domain. This resulted in $E_1(f)$, where E_1 is the energy spectrum and f is the frequency in hertz.

The spectra were transformed to the wavenumber domain using Taylor's hypothesis. Thus:

$$k = \frac{2\pi f}{U}, \tag{2}$$

where U is the mean velocity and k is the wavenumber. Following Lawn (1971), spectra were normalized using the relation

$$\bar{E}_1 = \frac{E(k_1)}{2\overline{u^2}R}, \tag{3}$$

and were plotted against $k_1 R$.

Although spectra were obtained at various radial positions, we only present centreline spectra for each principal experiment, as no significant variation with

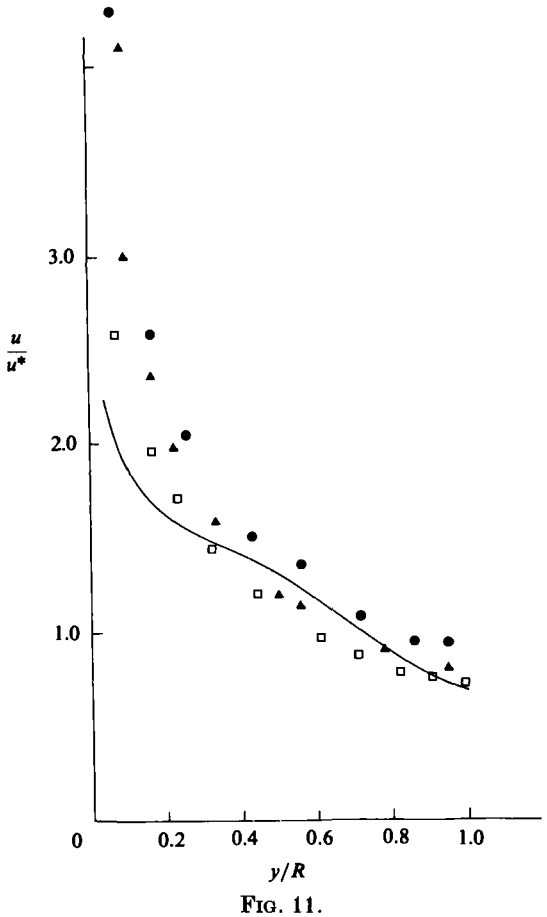

FIG. 11.

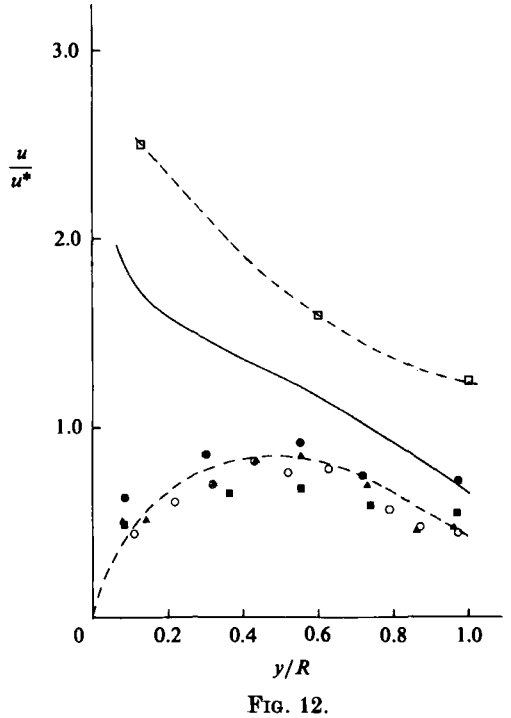

FIG. 12.

FIGURE 11. Axial turbulent intensities in fibre suspension at $Re = 5.3 \times 10^4$: ●, Pass 1 $DR = 54\%$; ▲, Pass 3 $DR = 47\%$; □, Pass 9 $DR = 40\%$; ——, water. 300 p.p.m. fibre + 150 p.p.m. polymer.

FIGURE 12. Axial turbulent intensities in mixed fibre/polymer suspension at $Re = 1.4 \times 10^4$: ●, Pass 1 $DR = 50\%$; □, Pass 2 $DR = 58\%$; ▲, Pass 3 $DR = 61\%$; ○, Pass 8 $DR = 59\%$; □, Pass 13 $DR = 40\%$; ——, water.

radial position was found. Thus in figures 14–17 we show the results for $Re = 1.4 \times 10^4$, 3.2×10^4 and 5.3×10^4 in fibre suspensions and at $Re = 1.4 \times 10^4$ in the fibre/polymer mixture. Our first results for spectra at $Re = 1.4 \times 10^4$ in fibre suspensions have been published, along with a correlation between the amount of drag reduction and the observed spectral shapes (McComb & Chan 1981). We shall discuss this below.

From figures 14–17, it can be seen that spectra measured in the fibre suspensions differ very markedly from the Newtonian spectrum. In particular, they are reduced below the Newtonian spectrum level over an intermediate range of wavenumbers (roughly corresponding to the inertial range). Also, there appear to be only differences of degree, rather than kind, between spectra measured in the fibre-like regime and those measured in the polymer-like regime. Nor are there any significant changes with Reynolds number.

In view of the results for mean and r.m.s. velocities, the latter two points are rather surprising. However, for the moment we shall concentrate on the important question of how one may interpret the reduced levels in these spectra.

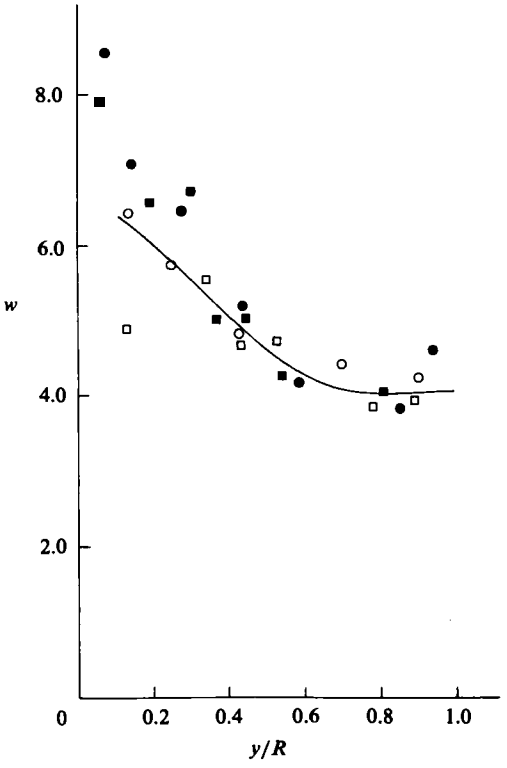

FIG. 13.

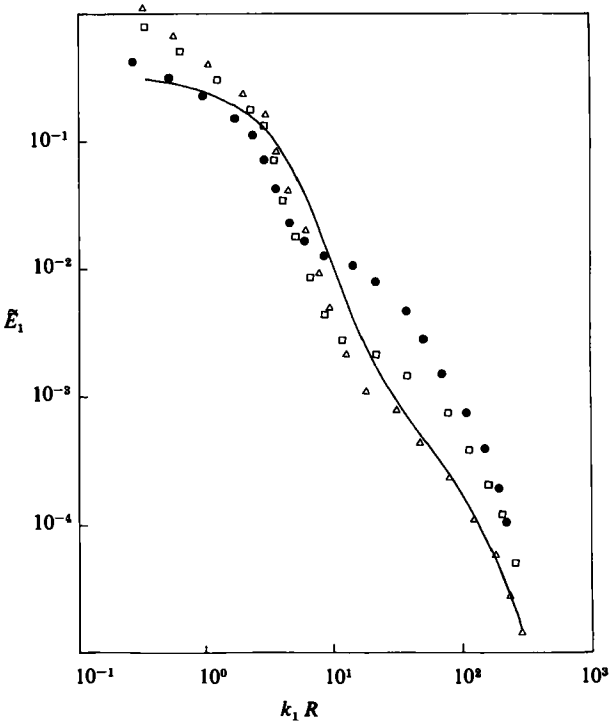

FIG. 14.

FIGURE 13. Distribution of r.m.s. transverse velocity in fibre suspension at $Re = 1.4 \times 10^4$: ■, Pass 1 $DR = 69\%$; ●, Pass 2 $DR = 76\%$; ○, Pass 3 $DR = 56\%$; □, Pass 5 $DR = 51\%$; ——, water. Fibre concentration 300 p.p.m.

FIGURE 14. One-dimensional energy spectra in fibre suspension at $Re = 1.4 \times 10^4$, $y/R = 1.0$: ●, Pass 1 $DR = 69\%$; □, Pass 2 $DR = 58\%$; △, Pass 3 $DR = 46\%$; ——, water. Fibre concentration 300 p.p.m.

Clearly it is here that the question of the relative contributions from fibres and from seeding particles, to the LDA signal, takes its most acute form. Without a firm answer to this question, our interpretation of spectra must necessarily be rather tentative. It seems that we must consider at least three possible interpretations of figures 14–17, and try to decide on their relative merits.

The three candidates are as follows:

(*a*) The LDA signal is mainly due to light scattered by the fibres, and the reduced spectrum level at intermediate wavenumbers reflects the inability of the fibres to follow the high-frequency motions of the turbulence.

(*b*) The LDA signal is mainly due to light scattered from the seeding particles. The spectrum in fibre suspensions is steeper than the Newtonian form because fibres inhibit energy transfer. The apparent recovery at high wavenumbers is due to a large fibre-induced noise level.

(*c*) The LDA signal is mainly due to light scattered from the seeding particles. The reduced level at intermediate wavenumbers is a 'dip' in the energy spectrum of the fluid due to resonant energy absorption by the fibres at wavenumbers near the inverse of the fibre length.

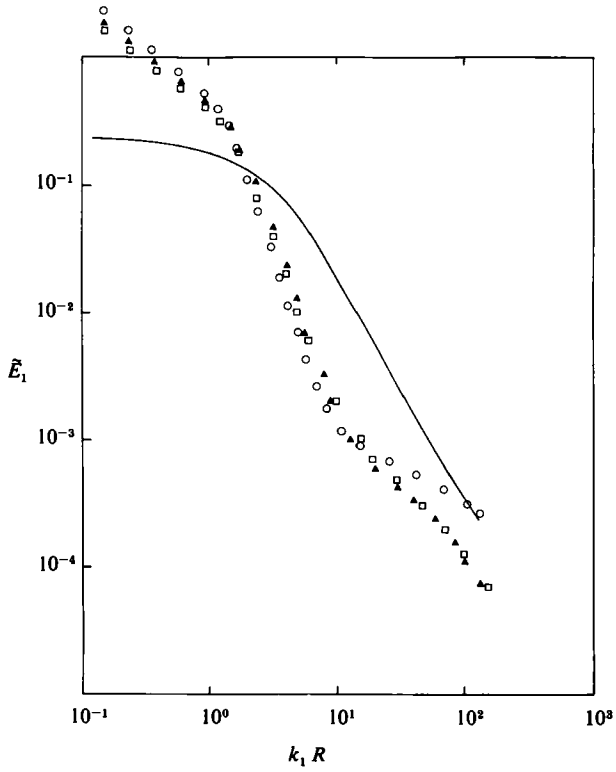

FIGURE 15. One-dimensional energy spectra in fibre suspension at $Re = 3.2 \times 10^4$, $y/R = 1.0$: ○, Pass 1 $DR = 71\,\%$; □, Pass 2 $DR = 62\,\%$; ▲, Pass 3 $DR = 58\,\%$; ——, water. Fibre concentration 300 p.p.m.

The first of these explanations seems to lack self-consistency. Quite apart from the fact that the fibres did not appear to contribute to the a.c. signal (see §3.2), it seems unreasonable to suppose that they would fail to follow the fluid motion at intermediate wavenumbers yet somehow manage to contribute at large wavenumbers.

In contrast, explanation (*b*) looks plausible. We have previously found S-shaped spectra in non-Newtonian polymer solutions (McComb *et al.* 1977), and these were attributed to a steeper 'fluid' spectrum superimposed on the broad-band 'noise' spectrum. In the present case, the more exaggerated shape could well be explained by a much higher noise spectrum due to the fibres. However, a close examination of the high-frequency region of each spectrum raises a question about this hypothesis. In all cases, the normalized spectra in fibre suspensions show a trend, with increasing wavenumber, to the result for water alone. In particular, from figure 14 we see that the spectrum for Pass 3 ($DR = 46\,\%$) at $Re = 1.4 \times 10^4$ becomes identical with that for water for $k_1 R$ greater than about 20. This apparent coincidence of normalized spectra implies that the supposed 'noise' spectrum scales on the mean-square turbulent intensity, which would seem to suggest that we are still observing the 'fluid' spectrum at the highest wavenumber shown.

Finally, we consider interpretation (*c*). Support for this view comes from the fact that the reduced spectrum level does actually occur at wavenumbers of the order of the inverse fibre length. This seems reasonably indicative of a dynamical interaction

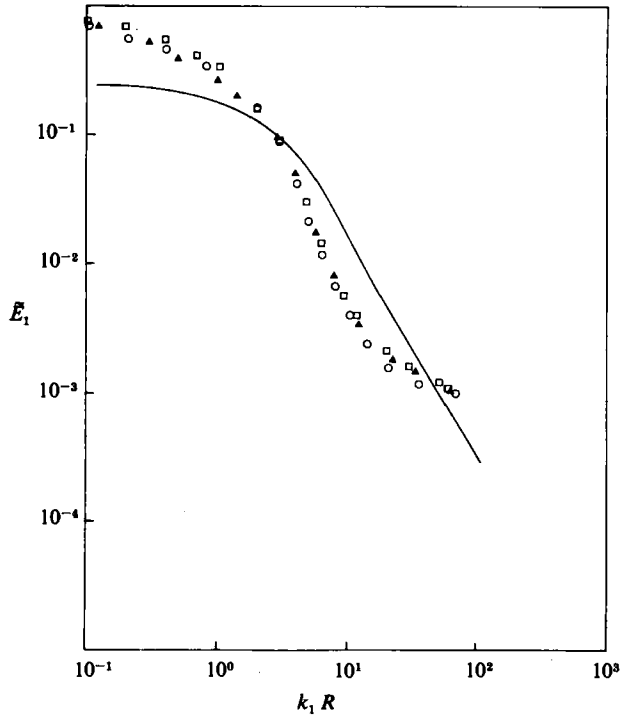

FIGURE 16. One-dimensional energy spectra in fibre suspension at $Re = 5.3 \times 10^4$, $y/R = 1.0$: ○, Pass 1 $DR = 54\%$; □, Pass 2 $DR = 52\%$; ▲, Pass 4 $DR = 46\%$; ——, water. Fibre concentration 300 p.p.m.

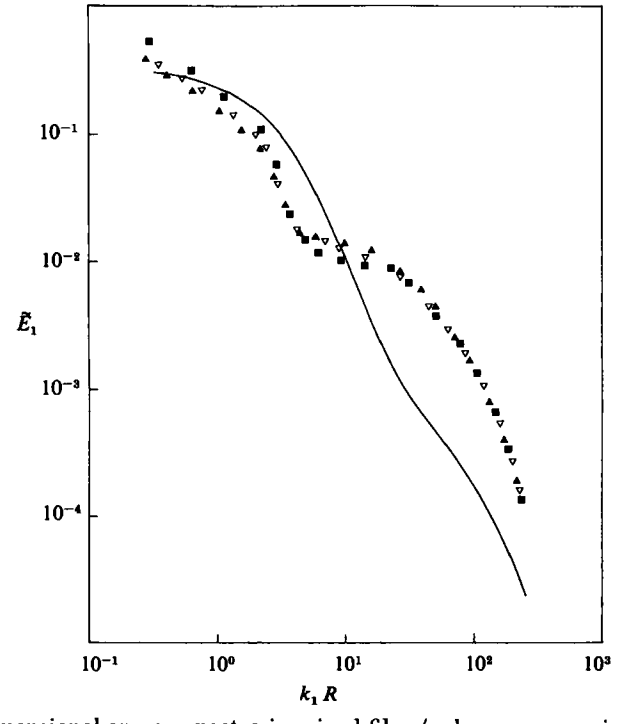

FIGURE 17. One-dimensional energy spectra in mixed fibre/polymer suspension at $Re = 1.4 \times 10^4$, $y/R = 1.0$: ■, Pass 2 $DR = 58\%$; ▲, Pass 3 $DR = 61\%$; ▽, Pass 4 $DR = 58\%$; ——, water. 300 p.p.m. fibre + 150 p.p.m. polymer (AP30).

between turbulent eddies and the individual fibres. Further, if we use these spectra to infer a lengthscale for the individual fibres, then it is possible to correlate the magnitude of the drag reduction with the inferred lengthscale. We have shown elsewhere (McComb & Chan 1982) that a relationship,

$$DR \times 100\,\% = \left\{0.70 \log_{10} \frac{l_{\mathrm{m}}}{D} - 2.60\right\} \times 100\,\%, \tag{4}$$

appears to hold for all the Reynolds numbers studied. Here D is the mean diameter of an individual fibre and l_{m} is the eddy–fibre interaction lengthscale. This was obtained by noting the two wavenumbers marking the beginning and end of the reduced region, taking the arithmetic mean to give the interaction wavenumber k_{m} and hence $l_{\mathrm{m}} = k_{\mathrm{m}}^{-1}$.

In all, therefore, our tentative conclusion is that the reduced level in the energy spectrum is probably due to resonant absorption of energy from turbulent eddies by individual fibres.

4.4. *Autocorrelations*

Autocorrelations of the streamwise velocity fluctuations were measured in order to obtain integral length- and timescales, as well as the mean period between bursts. Representative results for the autocorrelation coefficient $R_{11}(t)$ as a function of time, will be found in the thesis by Chan (1980). It was found that (with the exception of Pass 1 at $Re = 1.4 \times 10^4$) all the autocorrelations taken in fibre suspensions behaved much like those measured in drag-reducing polymer solutions (McComb & Rabie 1982). That is, when compared to the result for water, they had much higher values and persisted over much longer times.

The behaviour of R_{11} in Pass 1 at $Re = 1.4 \times 10^4$ was quite different. It fell off much more rapidly than in water for short lag times (virtually discontinuously), and thereafter decayed much more slowly than in water. This behaviour was also found in the 'undegraded' passes of the fibre/polymer mixture at $Re = 1.4 \times 10^4$. We concluded that this curious form of autocorrelation was characteristic of fibre-like drag reduction.

These results are summarized in a quantitative fashion in table 2 where we present the integral scales. The integral length- and timescales are defined by

$$L_{11} = \int_0^\infty R_{11}(r)\,\mathrm{d}r, \tag{5}$$

and

$$T_{\mathrm{E}} = \int_0^\infty R_{\mathrm{E}}(t)\,\mathrm{d}t. \tag{6}$$

Adopting Taylor's hypothesis, we can estimate L_{11} from (6) using the relation

$$L_{11} = UT_{\mathrm{E}}. \tag{7}$$

Referring to table 2, and taking results at the centreline, we see that passes 2 and 3 at $Re = 1.4 \times 10^4$ in the fibre suspension behaved like polymer solutions, showing greatly enhanced length- and timescales compared to the results for water ($T_{\mathrm{E}} = 2$ ms, $L_{11} = 5$ mm). In contrast, the results for Pass 1 showed only a small enhancement of the integral scales (disproportionately so, in view of the large percentage drag reduction). Again, undegraded passes in the fibre/polymer mixture behaved like Pass 1 in the fibre suspension at the same Reynolds number.

The mean period between bursts is an important parameter in studies of drag reduction. It may be obtained by measuring the autocorrelation with a short

			Lengthscale (mm)		Timescale (ms)	
$Re \times 10^{-4}$	Pass	DR (%)	$y/R = 0.3$	$y/R = 1.0$	$y/R = 0.3$	$y/R = 1.0$
1.4	1	69	15	7	18	5
	2	58	19	18	25	16
	3	46	18	17	19	15
3.2	1	71	40	80	25	32
	2	62	40	40	24	18
	3	58	30	10	19	14
5.3	1	54	20	20	7	5
	2	52	20	10	6	3
	4	46	20	10	6	2

(*a*) 300 p.p.m. fibre suspension

			Lengthscale (mm)		Timescale (ms)	
$Re \times 10^{-4}$	Pass	DR (%)	$y/R = 0.3$	$y/R = 1.0$	$y/R = 0.3$	$y/R = 1.0$
1.4	2	58	16	9	17	7
	3	61	16	8	18	6
	4	58	13	7	16	5

(*b*) 300 p.p.m. fibre suspension + 150 p.p.m. polymer solution

TABLE 2. Integral scales of the turbulence

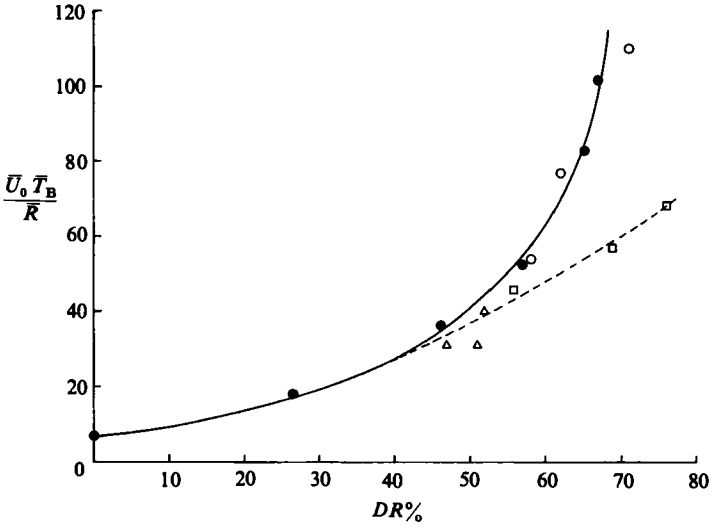

FIGURE 18. Variation of the mean time between bursts with the amount of drag reduction in fibre suspensions: □, fibre suspension $Re = 1.4 \times 10^4$; ○, fibre suspension $Re = 3.2 \times 10^4$; △, fibre suspension $Re = 5.3 \times 10^4$; ●, polymer solution $Re = 3.5 \times 10^4$ (McComb & Rabie 1982).

averaging time and estimating the bursting period T_B as the distance between peaks (Kim, Klein & Reynolds 1971; Strickland & Simpson 1975). The mean bursting period T_B is then obtained by repeating this process a number of times and averaging. The technique has been applied to drag-reducing polymer flows (Mizushima & Usui 1977; McComb & Rabie 1982).

In this work we calculated values of T_B from at least 30 samples. Elsewhere, as

few as 20 samples have been found satisfactory (see McComb & Rabie 1982). In figure 18 we plot $U_0 T_B/R$ against $DR\%$ (drag reduction) for $Re = 1.4 \times 10^4$, 3.2×10^4 and 5.3×10^4. As a basis for comparison, we also show results for a polymer solution at $Re = 3.5 \times 10^4$ (McComb & Rabie 1982). Two points may be noted. First, the results in the fibre suspensions for the two higher Reynolds numbers agree quite well with those taken in the polymer solution. Those in the fibre suspension for $Re = 1.4 \times 10^4$ do not. Secondly, for the case of $Re = 1.4 \times 10^4$ in the fibre suspension, there is no apparent change from fibre-like to polymer-like behaviour.

5. Conclusion

The present measurements confirm the preliminary results of McComb & Chan (1979) at $Re = 9.0 \times 10^3$. We have now shown that there is also a transition from a fibre-like to a polymer-like form of drag reduction at $Re = 1.4 \times 10^4$, as the fibre suspension degrades. However, at $Re = 3.2 \times 10^4$ and $Re = 5.3 \times 10^4$, this transition did not occur.

Thus for the two lower Reynolds numbers studied (9.0×10^3 and 1.4×10^4) it seems that there is a transition from fibre-like drag reduction in Pass 1 (or possibly Pass 2 as well) to polymer-like drag reduction in Pass 2 (or Pass 3) and the following passes.

The uncertainty here is a familiar problem in drag reduction with either polymers or fibres. Presumably improved mixing during Pass 1 sometimes offsets any degradation taking place. Whether this happens or not is an imponderable and is determined by solution/suspension preparation. For the sake of simplicity we shall assume in what follows that transition takes place between Pass 1 and Pass 2.

The so-called transition has the following features:

(*a*) In Pass 1, the mean velocity profile lies beyond the ultimate drag-reduction asymptote for polymers. In Pass 2 it lies in the polymer drag-reduction region. This is a weak criterion for a transition from fibre-like to a polymer-like drag reduction. Also, during Pass 1 the profile is close to the form for laminar flow.

(*b*) In Pass 1, the streamwise turbulent intensity is reduced (at least in some regions) below the value for water alone. In Pass 2 the streamwise intensity is everywhere very much larger than the value for water and in subsequent passes shows a trend back to the Newtonian result as the amount of drag reduction decreases. This is a strong criterion for a transition and the same is true of the two following criteria.

(*c*) The circumferential turbulent intensity behaves in the opposite way from the streamwise component. In Pass 1 it is increased above the level for water; in higher passes it is reduced below that level.

(*d*) The streamwise autocorrelation during Pass 1 is quite unlike that for water alone. Although its associated integral scales are somewhat larger than the result for water flow, it decays very much more rapidly at short times and then has a slowly varying 'tail' at longer times. Strictly, the use of a single integral scale to characterize this autocorrelation would be very misleading if taken on its own, without reference to the almost discontinuous change in shape. In contrast, the autocorrelation in Pass 2 (and higher passes) is very much like those found in polymer solutions.

At the two higher Reynolds numbers studied (3.2×10^4 and 5.3×10^4) the above features did not occur. Mean and r.m.s. velocity profiles, like autocorrelations, all lay in the polymer-like region. It should perhaps be emphasized that the difference between the higher and lower Reynolds numbers was not simply a matter of the amount of drag reduction. During Pass 1 at $Re = 3.2 \times 10^4$, the drag reduction was 71 %, which is much the same as (in some cases greater than) the drag reduction found in the fibre-like Pass 1 at $Re = 1.4 \times 10^4$.

Two further complications may be noted. First, one might suppose that, once the transition to polymer-like drag reduction had taken place, the results for the higher passes would be similar to results for the same percentage drag reduction at the higher Reynolds numbers. This was not the case. For example, mean velocity profiles for $Re = 9.0 \times 10^3$ and $Re = 1.4 \times 10^4$ showed a significant dependence on Reynolds number. In contrast, mean velocity profiles for $Re = 3.2 \times 10^4$ and $Re = 5.3 \times 10^4$ were the same at the same level of drag reduction. Further, at these higher Reynolds numbers, mean velocities and the mean time between bursts were very similar to values found in drag-reducing polymer solutions at the same level of drag reduction, whereas our results for $\overline{T}_B$ at 1.4×10^4 did not agree with the results for polymers.

Secondly, when we consider the results for spectra, we find no correspondence to the above picture. On the basis of our discussion in §4.3, all spectra show plain evidence of the presence of macroscopic fibres in the flow and are quite unlike the result for polymer solutions. Moreover, they show no real evidence of a transition from one kind of drag reduction to another – differences tend to be merely ones of degree. Further, if we infer interaction lengthscales from them, then we can correlate all the drag-reduction data, irrespective of either pass number or even Reynolds number.

Turning finally to the results for the mixed fibre/polymer suspension, we note that these (for Passes 1–8) are little different from those of Pass 1 in the pure fibre suspension, at the same Reynolds number. Accordingly, the only apparent effect of the polymers is to stabilize the fibre suspension against degradation. Of course the drag reduction obtained here (about 60 % during the undegraded passes) was smaller than that in the fibre suspension at $Re = 1.4 \times 10^4$ (about 69–76 %) and very much smaller than the maximum value (about 95 %) reported by Lee *et al.* (1974). Possibly if we had obtained drag reduction much greater than in the fibre suspension alone, some more distinctive evidence of a co-operative effect would have emerged.

The authors thank Dr P. Hutchinson of AERE, Harwell, for helpful advice on the interpretation of the LDA signal from a suspension containing macroscopic fibres. We also thank Turner Brothers Asbestos Co. Ltd for the drag-reducing Chrysotile asbestos suspensions.

REFERENCES

BERTSHY, J. R. & ABERNATHY, F. H. 1977 Modifications to laminar and turbulent boundary layers due to the addition of dilute polymer solutions. In *Proc. 2nd Int. Conf. on Drag Reduction, Paper* G1, *Cambridge*. BHRA.

BOBKOWICZ, A. J. & GAUVIN, W. H. 1967 *Chem. Engng Sci.* **22**, 229.

CHAN, K. T. J. 1980 Turbulent flow of drag-reducing fibre suspensions. Ph.D. Thesis, Edinburgh University.

EK, R., MOLLER, K. & NORMAN, B. 1979 The simultaneous measurement of velocity and concentration in fibre suspension flow. In *Dynamic Measurements in Unsteady Flows, Proc. Dynamic Flow Conference 1978, Marseille and Baltimore.*

ELLIS, H. D. 1970 *Nature* **226**, 352.

HOYT, J. W. 1972*a* *Trans. ASME* D: *J. Basic Engng* **94**, 258.

HOYT, J. W. 1972*b* *Naval Undersea Center Rep.* TP 299, *San Diego.*

HOYT, J. W. 1977 Polymer drag reduction – a literature review, 1975–76. In *Proc. 2nd Int. Conf. on Drag Reduction, Paper* A1, *Cambridge*. BHRA.

KEREKES, R. J. & GARNER, R. G. 1982 *Transactions Canadian Pulp and Paper Association*, September 1982, p. 53.

KIM, H. T., KLINE, S. J. & REYNOLDS, W. C. 1971 *J. Fluid Mech.* **50**, 133.

LAWN, C. J. 1971 *J. Fluid Mech.* **48**, 477.

LEE, W. K., VASELESKI, R. C. & METZNER, A. B. 1974 *AIChE J.* **20**, 128.

LITTLE, R. C., HANSEN, R. J., HUNSTON, D. L., KURI, O. K., PATTERSON, R. L. & TING, R. Y. 1975 *Ind. Engng Chem. Fund.* **14**, 283.

LOGAN, S. E. 1972 *AIAA J.* **10**, 962.

LUMLEY, J. L. 1969 *Ann. Rev. Fluid Mech.* **1**, 367.

MCCOMB, W. D., ALLAN, J. & GREATED, C. A. 1977 *Phys. Fluids* **20**, 873.

MCCOMB, W. D. & CHAN, K. T. J. 1979 *Nature* **280**, 45.

MCCOMB, W. D. & CHAN, K. T. J. 1981 *Nature* **292**, 520.

MCCOMB, W. D. & RABIE, L. H. 1982 *AIChE J.* **28**, 558.

MIZUSHIMA, T. & USUI, H. 1977 *Phys. Fluids Suppl.* **20**, S100.

MOYLS, A. L. & SABERSKY, R. H. 1978 *Intl J. Heat Mass Transfer* **21**, 7.

RADIN, I., ZAKIN, J. L. & PATTERSON, G. K. 1975 *AIChE J.* **21**, 358.

RUDD, M. J. 1972 *J. Fluid Mech.* **51**, 673.

SHARMA, R. V., SESHADRI, V. & MALHOTRA, R. C. 1979 *Chem. Engng Sci.* **34**, 703.

STRICKLAND, J. H. & SIMPSON, R. L. 1975 *Phys. Fluids* **18**, 306.

VIRK, P. S. 1975 *AIChE J.* **21**, 625.

VIRK, P. S., MICKLEY, H. S. & SMITH, K. A. 1970 *Trans. ASME* E: *J. Appl. Mech.* **37**, 488.

WICKRAMASINGHE, N. C. 1973 *Light Scattering Functions for Small Particles with Applications in Astronomy*. Bristol: Adam Hilger.